

Enhanced luminescence from $\text{Al}_x\text{Ga}_{1-x}\text{N}/\text{Al}_y\text{Ga}_{1-y}\text{N}$ quantum wells grown by gas source molecular beam epitaxy with ammonia

Sergey A. Nikishin^{*a}, Boris A. Borisov^a, Gregory A. Garrett^b, Wendy L. Sarney^b,
Anand V. Sampath^b, Hongen Shen^b, Michael Wraback^b, Mark Holtz^a.

^aNano Tech Center, Texas Tech University, Lubbock, TX, USA 79409;

^bU.S. Army Research Laboratory, AMSRD-ARL-SE-EM, Adelphi, MD, USA 20783

ABSTRACT

We report the structural and optical properties of $\text{Al}_x\text{Ga}_{1-x}\text{N}/\text{Al}_y\text{Ga}_{1-y}\text{N}$ quantum wells (QWs) structures grown by gas source molecular beam epitaxy with ammonia on sapphire (0001) substrates. QWs structures consist of five pairs of $\text{Al}_y\text{Ga}_{1-y}\text{N}$, $0.3 < y < 0.45$, wells (nominally 2-4 nm thick) and $\text{Al}_x\text{Ga}_{1-x}\text{N}$, $0.55 < x < 1$, barriers (nominally 5 nm thick). All the structures were completed with a 10 nm thick cap layer of AlN. We observed a significant enhancement in the cathodoluminescence intensities and longer photoluminescence lifetimes for QW structures grown in the 3D mode, as confirmed by spotty reflection high energy electron diffraction patterns. These effects are attributed to the formation of AlGaIn quantum dots in the well materials.

Keywords: AlGaIn quantum wells and dots, growth mode of quantum wells, time decay

1. INTRODUCTION

There has been significant progress in design and fabrication of the AlGaInN-based light emitting diodes (LEDs) operating below 300 nm [1, 2]. Emission wavelength as short as 210 nm has been recently reached [3]. AlGaInN LED structures are based on the well-known double-heterostructure design where a narrow-bandgap active region is sandwiched between two wider-bandgap *n*- and *p*-type layers. Despite the fact that AlGaInN alloys are direct bandgap semiconductors, LEDs based on these materials remain inefficient.

The active region of III-nitride LEDs is usually composed of a few pairs of GaN/InGaN or $\text{Al}_x\text{Ga}_{1-x}\text{N}/\text{Al}_y\text{Ga}_{1-y}\text{N}$ QWs. It is well known that the internal efficiency of InGaIn QWs is enhanced by formation of In-rich clusters [4], which behave like quantum dots (QDs) [5]. The localized states, obtained due to fluctuation of In content, protect carriers from recombining at nonradiative centers [6]. The carrier localization observed in wide bandgap AlGaInN [7] also was attributed to In segregation [8], leading to enhanced luminescence of these alloys. Kipshidze et al. [9] reported that adding of a small amount of In, less than 0.5%, to the GaN or $\text{Al}_{0.08}\text{Ga}_{0.92}\text{N}$ wells increases, by factor from 3 to 5, the luminescence intensity of QW structures. X-ray studies of these AlN/AlGaInN QWs signify formation of InGaIn regions in the well material despite very low In content [10]. QDs of InGaIn can be obtained by inducing Stranski-Krastanow growth mode [11]. A change from two dimensional (2D) to three dimensional (3D) growth mode can be reached by applying Si anti-surfactant [12] or by relying on residual strain in the well material [13]. Much less is known about $\text{Al}_x\text{Ga}_{1-x}\text{N}$ QDs [14]. Hirayama *et al.* [15] reported growth of $\text{Al}_x\text{Ga}_{1-x}\text{N}$ ($0.01 \leq x \leq 0.05$) QDs on $\text{Al}_{0.38}\text{Ga}_{0.62}\text{N}$ using Si anti-surfactant. However, they observed decreasing luminescence efficiency with increasing AlN content in the QD region.

Recently, it was shown that luminescence efficiency of $\text{Al}_{0.45}\text{Ga}_{0.55}\text{N}/\text{Al}_{0.55}\text{Ga}_{0.45}\text{N}$ QWs grown by gas source molecular beam epitaxy (GSMBE) with ammonia is very sensitive to the growth mode of a well material [16, 17]. It was shown that compositional inhomogeneity in plasma assisted MBE grown AlGaIn enhances luminescence efficiency due to formation of QD-like localized states inhibiting the movement of carriers to nonradiative sites [18].

In this paper we report the structural and optical properties of $\text{Al}_x\text{Ga}_{1-x}\text{N}/\text{Al}_y\text{Ga}_{1-y}\text{N}$ ($0.3 < x < 0.45$, $0.53 < y \leq 1$) QW structures using transmission electron microscopy (TEM) and room temperature CL and time-resolved photoluminescence (TRPL) measurements. We describe a significant improvement in the room temperature luminescence efficiency of $\text{Al}_x\text{Ga}_{1-x}\text{N}/\text{Al}_y\text{Ga}_{1-y}\text{N}$ QWs when the 3D growth mode is induced by reduced flux of NH_3 in

*sergey.a.nikishin@ttu.edu; phone 1 806 742-3530; fax 1 806 742-1245

the growth of well material. This intense emission is characterized by a long room-temperature lifetime comparable to that seen in low defect density GaN and suggests that spatial carrier localization enhances the luminescence efficiency. Our results, interpreted in terms of QD formation in well material, should result in improved quantum efficiency of LEDs operating below 300 nm.

2. EXPERIMENTS

2.1 Growth

The structures were grown by GSMBE with ammonia on (0001) sapphire substrates. Growth began with 30 minutes long nitridation of sapphire, at $\sim 900^\circ\text{C}$. Next, AlN(50 nm)/ Al_{0.68}Ga_{0.32}N (50 nm)/AlN (110 nm) buffer sandwich was grown to control the residual stress in an active region. The buffer was grown in 2D growth mode with 1x1 surface reconstruction as confirmed by streaky reflection high energy electron diffraction (RHEED) patterns. The growth continued with an active region consisting of five pairs of Al_xGa_{1-x}N ($0.3 < x < 0.45$) well and Al_yGa_{1-y}N ($0.53 < y \leq 1$) barrier. All Al_yGa_{1-y}N ($0.53 < y \leq 1$) barrier layers were grown in 2D growth mode, as demonstrated by the RHEED pattern of Fig. 1a. The thickness of the barriers was kept constant, 20 mono layers (MLs), in all experiments. The growth time of well material, Al_xGa_{1-x}N ($0.3 < x < 0.45$), was changed in the range from 21 s to 42 s which corresponded to deposition from ~ 8 MLs to ~ 16 MLs, respectively. Note the thickness of one ML of AlGa_{1-x}N is ~ 0.25 nm. Based on our previous results, QW structures were grown at the optimal temperature of $\sim 810^\circ\text{C}$ where deposition and evaporation rates of the well material are balanced [16, 17]. All the structures were completed with a 10 nm thick cap layer of AlN.

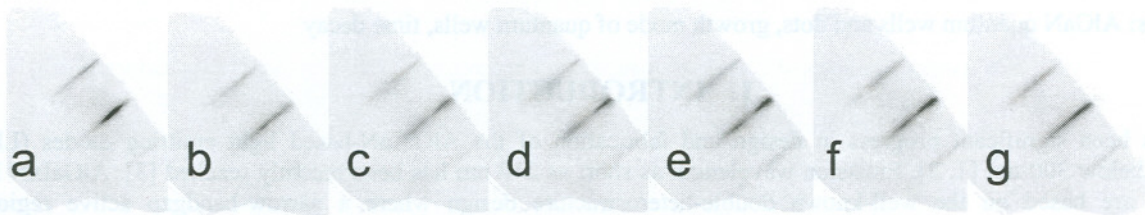


Fig. 1. Variation of the RHEED patterns during the growth. (a) 2D grown barrier at 20 sccm of ammonia; (b) onset of 2D to 3D transition of well at 6.5 sccm of ammonia; (c) – (f) 3D grown well at 6.25 sccm of ammonia after deposition of 4, 8, 12, 16 MLs, respectively; (g) onset of 3D to 2D transition of barrier on well at 20 sccm.

The ammonia flux used in the growth of wells was varied between 8 sccm and 5 sccm, in different structures. The growth mode of the well changes with reduced flux of ammonia. For example, 2D growth mode was maintained at ammonia fluxes greater than 7 sccm. At the ammonia flux of 6.5 sccm we observed weak splitting of 0th spot in the RHEED pattern after deposition of ~ 2 MLs (6 seconds of growth) of well material, Al_xGa_{1-x}N ($0.3 < x < 0.45$), as shown in Fig. 1b. With the ammonia flux reduced to 6.25 sccm the RHEED patterns become quite spotty after deposition from 4 MLs to 16 MLs of well material, as shown in Fig. 1 c-f. This behavior of the RHEED pattern is typical of growth mode change from 2D to 3D [19]. Well growth could not be continued for ammonia fluxes below 5 sccm. It should be noted that for all ammonia fluxes used for well growth the RHEED pattern of the barrier layer recovers within ~ 2 seconds, as shown in Fig. 1g, and shows 2D growth by the time the next well is grown. In other words the barriers are sufficiently thick for the growth to planarize the barrier surface before the next well is nucleated. This implies that any 3D grown islands are confined to individual wells. We refer this region as quantum well/quantum dot region. Note the varying RHEED patterns during the growth of wells with different thickness. As seen from Fig. 1b-c, approximately half of 2 nm thick well was grown under 2D growth mode. The 2.5 nm thick well should be composed of ~ 1 nm and ~ 1.5 nm of material grown in the 2D and 3D modes, respectively. Upon continued growth of the well to 3 and 4 nm thickness, the mechanism returns to 2D as illustrated in Fig. 1f-g. Thus, we expect the samples with 2.5 nm thick well to have the highest density of isolated 3D islands within the well. Although the detailed mechanism of 3D islands formation, their density and shape are still under investigations, we believe it is similar to reported by Han *et al.* [20] where the GaN and AlGa_{1-x}N QDs were grown using liquid droplet epitaxy.

2.2 Transmission electron microscopy.

Figure 2 shows a TEM cross-section of the $\text{Al}_x\text{Ga}_{1-x}\text{N}/\text{Al}_y\text{Ga}_{1-y}\text{N}$ quantum well/quantum dot region. The sample was imaged with a JEOL 2010F TEM operated at 200 keV. The image was taken along the $[11\bar{2}0]_{\text{film}}/[1\bar{1}00]_{\text{substrate}}$ zone axis. The darker contrast is indicative of the strain field around the quantum dots, but the embedded dots do not generate dislocations in the surrounding quantum wells. We do see an apparent increase in the lattice constant within the dots along the growth direction. There is very little contrast between the actual dots and the surrounding matrix, therefore it is difficult to obtain precise dimensions. This is due to the relatively small difference in chemical composition between the dots and the well, and from the averaging of information along the beam direction. Despite the apparent difficulties in obtaining TEM images of the quantum dots, we take this as corroborating evidence consistent with the RHEED data described above and the optical measurements below.

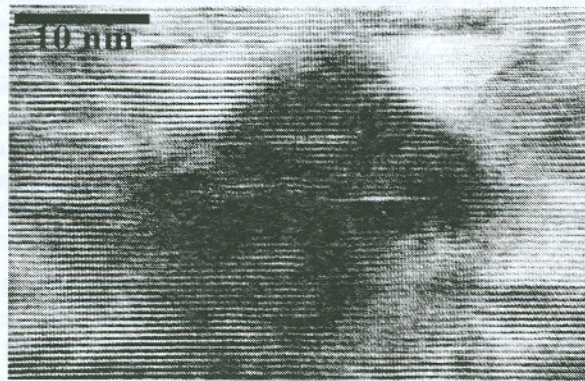


Fig. 2. TEM cross section of $\text{Al}_{0.45}\text{Ga}_{0.55}\text{N}/\text{Al}_{0.58}\text{Ga}_{0.42}\text{N}$ QW/QD region.

2.3 Cathodoluminescence.

The dependence of CL intensity versus ammonia flux for the set of QW structures grown at 810°C is shown in Fig. 3. The growth time of the well material was held constant and ammonia flux was varied from 5 to 8 sccm in different experiments. A maximum CL intensity was obtained at ammonia flux of 6.50 ± 0.25 sccm.

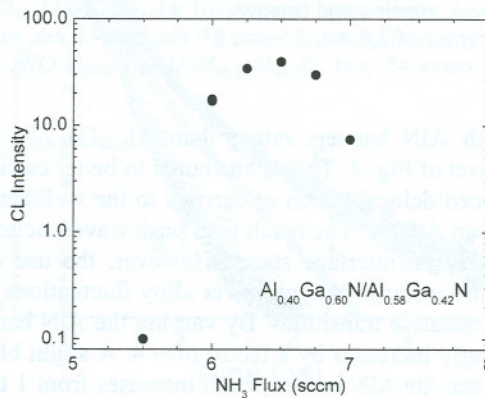


Fig. 3. The room temperature CL intensity of $\text{Al}_{0.40}\text{Ga}_{0.60}\text{N}/\text{Al}_{0.58}\text{Ga}_{0.42}\text{N}$ QWs versus ammonia flux.

Varying the ammonia flux results in differences in the well material formation. At low ammonia flux the evaporation of Ga dominates resulting in low growth rate—smaller well thickness—and increased Al content. We found that at low ammonia flux, < 5 sccm, there was no deposition of well material and the CL originates from the barrier material. At high ammonia flux, > 7 sccm, we observe 2D growth in the well and barrier, as described above, and low CL intensity. In the intermediate regime, where the CL intensity shows a maximum, 3D growth is observed consistent with the formation of islands or quantum dots in the well region. The CL intensity is observed to be very sensitive to even small changes in ammonia flux in this intermediate regime, exhibiting enhancement by a factor of ~ 40 between fluxes of 5.5 and 6.5 sccm before rapidly diminishing when flux is increased from 6.5 to 7.0 sccm. This enhancement in CL intensity with ammonia flux is attributed to the formation of isolated quantum dots in the well material [16, 17]. These quantum dots will localize excited carriers and enhance radiative recombination.

The intensity of CL is found to depend strongly on well thickness, as seen in Fig. 4. In quantum wells grown under 2D conditions, i.e. without quantum dots, the polarization field plays a strong role in delocalizing electrons and holes thereby diminishing the radiative emission. In our experiments, the highest intensity for $\text{Al}_{0.40}\text{Ga}_{0.60}\text{N}/\text{Al}_{0.58}\text{Ga}_{0.42}\text{N}$ QWs was measured when the growth time of well material was 26 seconds, curve 2 in Fig. 4, corresponded to 2.5 nm thick wells. We note, however, that the intensity from samples with thicker wells is high compared with pure 2D grown quantum wells. Evidently, the presence of quantum dots plays an important role in luminescence even for these thicker wells. The intensity dependence observed for the spectra in Fig. 4 are correlated with measured PL lifetimes discussed below. The dependence seen for the $\text{Al}_{0.40}\text{Ga}_{0.60}\text{N}/\text{Al}_{0.58}\text{Ga}_{0.42}\text{N}$ series (1–4) may be attributed to changes in carrier confinement to the QD regions. Evidently, samples with 2.5 nm thick possess the best quantum dots, consistent with the RHEED data in Fig. 1.

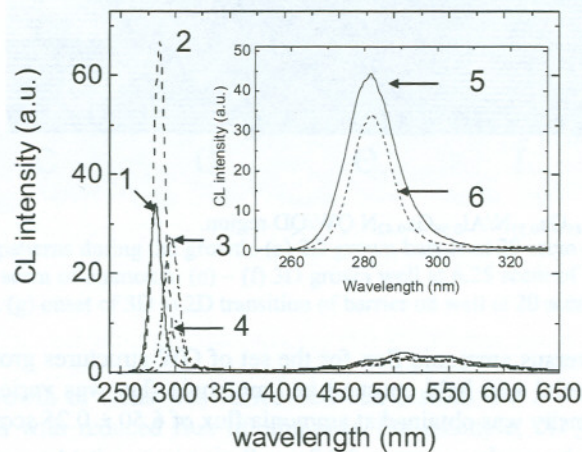


Fig. 4. The room temperature CL peak position and intensity of $\text{Al}_{0.4}\text{Ga}_{0.6}\text{N}/\text{Al}_{0.58}\text{Ga}_{0.42}\text{N}$ QWs. Spectra 1, 2, 3, and 4 correspond to expected well thickness of 2.0 nm, 2.5 nm, 3.0 nm, and 4.0 nm, respectively. The inset shows the main peak of $\text{Al}_{0.40}\text{Ga}_{0.60}\text{N}/\text{AlN}$ QW, curve #5, and $\text{Al}_{0.40}\text{Ga}_{0.60}\text{N}/\text{Al}_{0.58}\text{Ga}_{0.42}\text{N}$ QW, curve #6, corresponding to the well thickness of 2 nm.

Turning to the structures grown with AlN barriers rather than $\text{Al}_{0.58}\text{Ga}_{0.42}\text{N}$, we observe ~ 30% increase in the luminescence intensity, as shown in inset of Fig. 4. This is attributed to better carrier confinement in the wells. A second factor to consider is polarization-induced delocalization of carriers to the well/barrier interfaces. This effect is stronger when using pure AlN barriers rather than AlGa_{0.6}N. The result is to push wavefunctions further into the barriers, enhancing non-radiative recombination through barrier/interface states. However, the use of a pure AlN barrier may have the advantage of reducing the density of these states through lower alloy fluctuations at the interface, with the net result of reduced competition with the desired radiative transitions. By varying the AlN barrier width from 1 to 5 nm (not shown here) we found that CL intensity strongly increases by a factor of ~ 4. A slight blue shift, by ~ 40 meV, is observed in the CL peak position for this series when the AlN barrier width increases from 1 to 5 nm. These effects can likewise be attributed to improving carrier confinement by thicker barriers and subsequent radiative recombination efficiencies. A similar effect was observed for QW structures where the composition of well material was varied between 0.30 and 0.45. The formation of quantum dots in the well region appears to enhance the CL intensity in our samples. An associated

effect on the PL lifetime is also expected due to changes in the carrier capture and recombination dynamics. We now describe the PL studies.

2.4 Time resolved photoluminescence.

To investigate the carrier recombination dynamics of the samples, time-resolved photoluminescence was performed. The observed lifetimes in these QWs is expected to be affected by bulk defects, interface states, carrier localization in the QDs, and wave function separation due to the piezoelectric field and polarization effect in the *c*-axis growth direction. A time-correlated single photon counting (TCSPC) technique [18] was used with a microchannel plate photomultiplier with ~25 ps resolution. The pump excitation source was a doubled optical parametric amplifier giving sub-100 fs pulses at 250 nm.

Shown in Fig. 5 are data for four samples taken with a pump fluence of ~0.72 $\mu\text{J}/\text{cm}^2$. Three samples correspond to $\text{Al}_{0.40}\text{Ga}_{0.60}\text{N}/\text{Al}_{0.58}\text{Ga}_{0.42}\text{N}$ with well thickness of 2.0, 2.5, and 4.0 nm, labeled 1, 2, and 4 in association with CL spectra in Fig. 4. The corresponding measured $1/e$ lifetimes are 150, 223, and 120 ps, respectively. The longest lifetime is consistent with the highest CL intensity. For the 2.0 nm well, the growth time is insufficient to form well-defined quantum dots resulting in a shorter lifetime, similar to standard superlattices of these materials, and weaker luminescence. At 2.5 nm well thickness, the quantum dots are well formed as illustrated by the RHEED data (Fig. 1 b-e). The observed increase in lifetime and CL intensity enhancement may thus be attributed to localization of carriers to the QD regions away from nonradiative recombination centers. When thicker (4.0 nm) wells are grown, the longer growth time permits formation of a smoother 2D morphology as seen from the RHEED (Fig. 1 f-g). As a result, the quantum dots play little role in the recombination process showing shorter PL lifetime and lower CL intensity. This underscores the importance of the well thickness in utilizing quantum dots to enhance light emission in AlGaIn superlattices.

We also show in Fig. 5 the PL decay for an $\text{Al}_{0.40}\text{Ga}_{0.60}\text{N}/\text{AlN}$ sample with 2.0 nm well thickness, corresponding to CL spectrum 5 in Fig. 4. This sample was found to show greatly enhanced CL intensity over those grown with the alloy barriers, an effect we attributed to improved confinement of carriers in the wells. We see a PL decay lifetime of ~320 ps. The similar structure with AlGaIn barrier had a significantly shorter lifetime of 150 ps. These results confirm the expected result that the AlN barriers are superior for carrier confinement enhancing the luminescence efficiency. We note that it is possible a 2.5 nm well with AlN barriers would exhibit superior properties in lifetime and intensity, since this thickness was superior in the case of $\text{Al}_{0.40}\text{Ga}_{0.60}\text{N}/\text{Al}_{0.58}\text{Ga}_{0.42}\text{N}$ quantum well structures. This suggestion is under investigation.

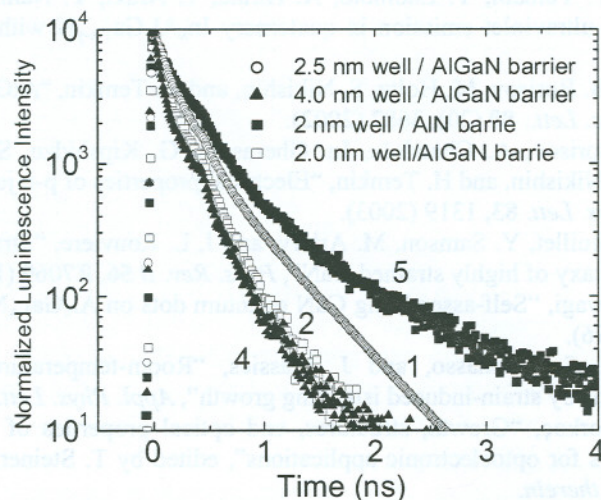


Fig. 5. Room-temperature time-resolved photoluminescence of $\text{Al}_{0.4}\text{Ga}_{0.6}\text{N}$ QWs with AlN or $\text{Al}_{0.58}\text{Ga}_{0.42}\text{N}$ barriers. Lines show best fit to a double exponential decay convoluted with the system response of ~25 ps.

3. CONCLUSIONS

In summary, we observe a significant increase in the deep UV CL and PL emission from QW structures of AlGaInN. The increase is attributed to the formation of quantum dots within the wells. For $\text{Al}_{0.40}\text{Ga}_{0.60}\text{N}/\text{Al}_{0.58}\text{Ga}_{0.42}\text{N}$ structures we observed that well thickness of 2.5 nm exhibits quantum dot formation as evidenced by 3D growth using *in situ* RHEED measurements. We observe the greatest CL intensity and longest PL lifetime for these $\text{Al}_{0.40}\text{Ga}_{0.60}\text{N}/\text{Al}_{0.58}\text{Ga}_{0.42}\text{N}$ structures with this well thickness. By replacing the barriers with pure AlN we observe further enhancement of both the CL intensity by $\sim 30\%$ and PL lifetime by a factor of 2. We interpret these observations in terms of formation of quantum well/quantum dot regions in $\text{Al}_x\text{Ga}_{1-x}\text{N}/\text{Al}_y\text{Ga}_{1-y}\text{N}$ ($0.3 < x < 0.45$, $0.53 < y \leq 1$) QW structures.

ACKNOWLEDGMENTS

TTU team acknowledges support from NSF (ECS-0304224 and ECS-0609416), THECB-ARP-003644-0014-2006, and the J. F Maddox Foundation.

REFERENCES

1. J. Zhang, X. Hu, A. Lunev, J. Deng, Yu. Bilenko, T. M. Katona, M. S. Shur, R. Gaska, and M. A. Khan, "AlGaIn Deep-Ultraviolet Light-Emitting Diodes", *Jap. J. Appl. Phys.* **44**(10), 7250-7253 (2005), and references therein.
2. S. A. Nikishin, B. Borisov, V. Kuryatkov, M. Holtz, A. Usikov, V. Dmitriev, and H. Temkin, "Deep UV AlGaIn light emitting diodes grown by gas source molecular beam epitaxy on sapphire and AlGaIn/sapphire substrates," *Proc. SPIE*, **6121**, 61210T-1-16 (2006), and references therein.
3. Y. Taniyasu, M. Kasu, and T. Makimoto, "An aluminium nitride light-emitting diode with a wavelength of 210 nanometres", *Nature*, **441**(18), 325-328 (2006).
4. S. Nakamura, "InGaIn-based violet laser diodes", *Semicond. Sci. Technol.* **14**, R27 (1999).
5. K. P. O'Donnell, R. W. Martin, and P. G. Middleton, "Origin of luminescence from InGaIn diodes", *Phys. Rev. Lett.* **82**(1), 237 (1999).
6. S. F. Chichibu, H. Marchand, M. S. Minsky, S. Keller, P. T. Fini, J. P. Ibbetson, S. B. Fleischer, J. S. Speck, J. E. Bowers, E. Hu, U. K. Mishra, S. P. DenBaars, T. Deguchi, T. Sota, and S. Nakamura, "Emission mechanisms of bulk GaN and InGaIn quantum wells prepared by lateral epitaxial overgrowth," *Appl. Phys. Lett.*, **74**, 1460 (1999).
7. M. Y. Ryu, C. Q. Chen, E. Kuokstis, J. W. Yang, G. Simin, and M. Asif Khan, "Luminescence mechanisms in quaternary $\text{Al}_x\text{Ga}_y\text{In}_{1-x-y}\text{N}$ materials", *Appl. Phys. Lett.* **80**, 3730 (2002).
8. H. Hirayama, A. Kinoshita, T. Yamabi, Y. Enomoto, A. Hirata, T. Araki, Y. Nanishi, and Y. Aoyagi, "Marked enhancement of 320–360 nm ultraviolet emission in quaternary $\text{In}_x\text{Al}_y\text{Ga}_{1-x-y}\text{N}$ with In-segregation effect", *Appl. Phys. Lett.* **80**, 207 (2002).
9. G. Kipshidze, V. Kuryatkov, B. Borisov, M. Holtz, S. Nikishin, and H. Temkin, "AlGaInN-based ultraviolet diodes grown on Si (111)", *Appl. Phys. Lett.*, **80** (20), 3682 (2002).
10. V. Kuryatkov, K. Zhu, B. Borisov, A. Chandolu, Iu. Gherasoiu, G. Kipshidze, S. N. G. Chu, M. Holtz, Yu. Kudryavtsev, R. Asomoza, S. Nikishin, and H. Temkin, "Electrical properties of p-n junctions based on superlattices of AlN/AlGa(In)N", *Appl. Phys. Lett.* **83**, 1319 (2003).
11. B. Daudin, F. Widmann, G. Feuillet, Y. Samson, M. Arlery, and J. L. Rouviere, "Stranski-Krastanov growth mode during the molecular beam epitaxy of highly strained GaN", *Phys. Rev. B* **56**, R7069 (1997).
12. S. Tanaka, S. Iwai, and Y. Aoyagi, "Self-assembling GaN quantum dots on $\text{Al}_x\text{Ga}_{1-x}\text{N}$ surfaces using a surfactant", *Appl. Phys. Lett.* **69**, 4096 (1996).
13. B. Damilano, N. Grandjean, S. Dalmaso, and J. Massies, "Room-temperature blue-green emission from InGaIn/GaN quantum dots made by strain-induced islanding growth", *Appl. Phys. Lett.*, **75**, 3751 (1999).
14. D. Huang, Y. Fu, and H. Morkoç, "Growth, structures, and optical properties of III-nitride quantum dots", in "Semiconductor nanostructures for optoelectronic applications", edited by T. Steiner, Artech House, Inc., Boston-London, 2004, and references therein.
15. H. Hirayama, Y. Aoyagi, and S. Tanaka, "Fabrication of self-assembling AlGaIn quantum dot on AlGaIn surfaces using anti-surfactant", *MRS Internet J. Nitride Semicond. Res.* **4S1**, G9.4 (1999).
16. B. Borisov, S. Nikishin, V. Kuryatkov, and H. Temkin, "Enhanced deep ultraviolet luminescence from AlGaIn quantum wells grown in the three dimensional mode", *Appl. Phys. Lett.* **87**, 191902 (2005).

17. B. A. Borisov, S. A. Nikishin, V. V. Kuryatkov, V. I. Kuchinski, M. Holtz, and H. Temkin, "Enhanced radiative recombination in AlGaIn quantum wells grown by molecular-beam epitaxy", *Semiconductors*, **40**, 454 (2006).
18. C. J. Collins, A. V. Sampath, G. A. Garrett, W. L. Sarney, H. Shen, M. Wraback, A. Yu. Nikiforov, G. S. Cargill III, and V. Dierolf, "Enhanced room-temperature luminescence efficiency through carrier localization in Al_xGa_{1-x}N alloys", *Appl. Phys. Lett.* **86**, 031916 (2005).
19. See for example, M. B. Panish and H. Temkin, *Gas Source Molecular Beam Epitaxy*, Springer-Verlag, Berlin, 1993.
20. J. Han, <http://www.eng.yale.edu/faculty/vita/han-projects.htm>